GA-FEM Method for Optimum Current Search for Torque Ripple Mitigation in Nonsinusoidal PMSM and Analysis of On-load Parameters

Allan Gregori de Castro*, Celio Corrêa Lemes Filho†, Luiz Henrique Reis de Jesus†,
William César de Andrade Pereira‡, Geyverson Teixeira de Paula †
and José Roberto Boffino de Almeida Monteiro *
*São Carlos School of Engineering, Department of Electrical and Computing Engineering
University of São Paulo, São Carlos, São Paulo, Brazil
allangregori@gmail.com, jrm@sc.usp.br
‡WEG Drives & Controls, Jaraguá do Sul, Santa Catarina, Brazil
williamwcap@gmail.com
†School of Electrical, Mechanical and Computer Engineering
Federal University of Goiás, Goiânia, Goiás, Brazil
eng.celiofilho@gmail.com, luizhenriqueengineer@gmail.com, geyverson@gmail.com

***Abstract*—Permanent magnet synchronous motors with spatial harmonics can develop significant torque ripple under sinusoidal stator current feeding strategy. Usual approaches to reduce torque ripple aim the design of stator current harmonics, based on the machine electrical parameters, to induce compensating torque pulsations. However, the machine parameters are highly dependent on the electric load and the current harmonic content. Thus, these dependencies impose a challenge on the search for optimum stator currents. To overcome this drawback, this paper presents a genetic algorithm (GA) optimum current search procedure based on the machine design assisted by the Finite Element Method (FEM). Additionally, the variation of the on-load estimated electrical parameters is analyzed considering different current feeding strategies. The results demonstrate that, according to FEM analysis, a null torque ripple with an increased torque per Ampère ratio is achieved and the parameter analysis demonstrates their different variation according to the current strategy.**

***Keywords* – Finite element method, Genetic algorithm, Permanent Magnet Synchronous Motor, Torque ripple mitigation.**

I. Introduction

Features like high efficiency and high power density have made the Permanent Magnet Synchronous Motors (PMSMs) an interesting candidate to be used in a large range of applications, from compressors in household appliances to traction in electrical vehicles [1]–[3]. Ideally, the PMSM presents sinusoidal permanent magnet (PM) flux linkage distribution and inductance waveforms. In this way, sinusoidal stator currents are able to provide smooth torque independent of rotor position. However, as a result of design guidelines or even mechanical tolerances in the manufacturing process, the machine may exhibit important magnitudes of cogging torque and spatial harmonics in PM flux linkage and inductances. The interaction of spatial harmonics and sinusoidal stator current can produce significant parasitic torque pulsations. The main consequences of torque pulsations include the increase of vibration, acoustic noise, and speed oscillation, which are important concerns in numerous applications [3]–[6].

The efforts to reduce torque ripple in PMSM drives presented in the literature can be divided into machine design-based and control-based approaches [6]. The machine design-based approach usually focuses in improve the stator or rotor design to reduce the harmonic content on inductances, PM flux and cogging torque. The optimization of mechanical parameters encounters limitations in terms of cost and manufacturing complexity. Also, it is difficult to achieve a robust design since small geometry variations in the manufacturing process, e.g., mechanical tolerances, can have a significant impact on torque ripple amplitude [7], [8].

On the other hand, recognizing that the torque pulsations come from the interaction of stator current with machine spatial harmonics, the goal of control-based approaches is to design and implement proper harmonic stator current to compensate the pulsating torque components. These approaches can substantially reduce torque ripple by, usually, updating the current references and control algorithms.

Several publications have appeared over the last decades documenting methods to define optimum feeding strategy for torque ripple mitigation in PMSM drives. In [9], a genetic algorithm (GA) based method is employed to optimize the magnitude and phase of selected current harmonics in direct and quadrature axis in a PMSM with nonsinusoidal back electromotive force (back-EMF). In [10], a GA method is used to search an optimized current considering the zero sequence back-EMF harmonics to contribute in torque production. In these studies, the machine saturation and load effect on machine parameters are not taken into account in the current design, reducing the effectiveness of torque ripple mitigation

https://doi.org/10.53316/sepoc2021.026

with minimum stator current magnitude requirement. In [11] the inductance saturation is included in an analytical solution for optimum harmonic current design. However, it is considered the machine parameters varying according to sinusoidal currents. As demonstrated in [12]–[14], nonsinusoidal currents can produce different deformation on the inductance, PM flux and cogging torque waveform.

In this scenario, this paper firstly proposes a search method using GA assisted by Finite Element Analysis (FEA) of a PMSM to design and map optimized current waveforms independently of machine electrical parameters, aiming torque ripple mitigation with minimum stator current requirement, i.e., smooth torque production with Maximum Torque per Ampère (MTPA).

Besides the current optimization, electrical parameter analysis and mapping is of importance in many aspects, including its usage for observers, model based controllers and MTPA algorithms. Among the electrical parameters, this paper focuses on the analysis of self and mutual inductances for different current supply conditions, including sinusoidal currents and those designed by the GA method aiming the investigation and analysis of the impact of current magnitude and waveform on parameters variation.

The contributions of this paper can be summarized as follows:

1) Design of optimized currents for torque ripple mitigation using a proposed GA method assisted by FEA. The optimized current is obtained considering the scenario with and without the possibility of circulating zero sequence current. Further, an analysis is carried out comparing the obtained solutions to conventional current waveforms.
2) Analysis of the on-load inductance variations for different load conditions with different current waveforms, including saturation region.

II. ELECTROMAGNETIC TORQUE IN PMSMS

Numerous methods have been presented and verified in the literature for accurate electromagnetic torque calculation in electrical machines [15]. Among these methods, the Maxwell Stress Tensor (MST) method in FEA stands out for its ease of implementation and good agreement with experiments [15].

In MST, the total torque $T_e \in \mathbb{R}$ produced by a PMSM can be calculated by

$$T_e = \frac{l_{fe} r^2}{\mu_0} \int_0^{2\pi} (\vec{B}_{OP})_R \times (\vec{B}_{OP})_T d\theta \qquad (1)$$

where $l_{fe} \in \mathbb{R}_+$ is the active axial length of the electrical machine, $\mu_0 \in \mathbb{R}_+$ is the permeability of free space, $r \in \mathbb{R}_+$ is the radius associated with the middle of the air gap, $\theta \in \mathbb{R}$ is the angular position in air gap, $(\vec{B}_{OP})_R \in \mathbb{R}^3$ is the radial component of flux density of the operation point and $(\vec{B}_{OP})_T \in \mathbb{R}^3$ is the tangential component of flux density of the operation point calculated at the middle of the air gap. Further than the calculation of electromagnetic torque, (1) supports improved parameter estimation methods, as presented in the following.

A. On-load machine parameters calculation

The estimation of machine electrical parameters is of importance in many aspects of control schemes, including the design and implementation of controllers, state observers/estimators, torque calculation, MTPA algorithms and torque ripple mitigation strategies. The parameters usually required for a PMSM electrical model are: phase resistance, self and mutual inductances, derivatives of self and mutual inductances, PM flux linkage and derivatives of PM flux linkage. Among these parameters, those related to inductance and PM flux linkage can be obtained by conventional FEA from the machine design. However, due to numerical errors or distortions on the waveforms due to nonsinusoidal current circulation, the conventional local differentiation operation for the calculation of inductances and PM-flux linkage derivatives may lead to significant inaccuracies. To overcome this problem, improved calculation methods were recently presented in the literature, based on MST and Frozen Permeability Method (FPM) for the calculation of back-EMF [12], inductance derivatives [13], and cogging torque [16].

Focusing on the inductance parameter analysis through FEA, the recently proposed improved method in [13], based on MST a FPM, for accurate inductance derivative calculation yields to

$$\frac{dL_{xy}(\theta_e, \vec{i})}{d\theta_e} = \frac{2 l_{fe}}{n_p i_x i_y \mu_0 (r_o - r_{in})} \int_S r (\vec{B}_{x,\vec{i}})_R \times (\vec{B}_{y,\vec{i}})_T \, d\vec{S} \qquad (2)$$

where $L_{xy}(\theta_e, \vec{i}) \in \mathbb{R}$, with x and y referring to phase 'a', 'b' or 'c', is the self inductance parameter of phase x when $x = y$ and the mutual inductance parameter between phase x and y when $x \neq y$. The inductance terms are expressed as a function of electrical rotor position $\theta_e \in \mathbb{R}$ and stator current vector $\vec{i} = \langle i_a, i_b, i_c \rangle$, since the dependency of load condition. $r_o \in \mathbb{R}_+$ and $r_{in} \in \mathbb{R}_+$ are the outer and inner radius of the air gap and S is the cross-sectional area of the air gap with normal vector $\vec{S} \in \mathbb{R}^3$. $\vec{B}_{x,\vec{i}} \in \mathbb{R}^3$ and $\vec{B}_{y,\vec{i}} \in \mathbb{R}^3$ are the phase flux density contributions due to stator currents.

III. GA BASED OPTIMUM CURRENT SEARCH METHOD FOR TORQUE RIPPLE MITIGATION

Genetic algorithms are stochastic based search algorithms, widely used as optimization method for solving constrained/unconstrained, nondifferentiable, discontinuous or nonlinear problems [7], [9], [10], [17], [18]. The GA algorithm is inspired on the mechanics of natural selection, the process that drives biological evolution. In GA, the solution candidates for the optimization problem are called individuals of a population. In each step, called generation, the GA evaluate the fitness of the individuals in the sense of producing best solutions, and those that best perform have more chance to survive or to be selected to produce a new population for the next generation. Over successive generations, the population evolves toward an optimum solution.

In this section, the GA is employed to search for the optimum current waveform to mitigate torque ripple of a PMSM

with minimum required current magnitude. Specifically, the proposed approach extensively execute the GA algorithm in a set of rotor positions, covering the machine electric cycle. For a given rotor position θ_e, the kth individual $\vec{I}_k(\theta_e)$ of a population of size $P \in \mathbb{N}^*$ have the format of

$$\vec{I}_k(\theta_e) = \langle i_{a,k}(\theta_e), i_{b,k}(\theta_e), i_{c,k}(\theta_e) \rangle \tag{3}$$

where

$$\vec{I}_k(\theta_e) \in \boldsymbol{M} \tag{4}$$

such that $\boldsymbol{M}$ is the search space given by

$$\boldsymbol{M} = \{\langle m, n, o \rangle \in \mathbb{R}^3 | -I_{max} \leq m, n, o \leq I_{max}\} \tag{5}$$

where $I_{max} \in \mathbb{R}_+$ is the limit of search space.

The first aimed objective $f_1(\vec{I}_k(\theta_e), \theta_e) \in \mathbb{R}_+$ of the optimization process is that the solution must produce the required torque $T_e^{ref} \in \mathbb{R}$ for each θ_e, which can be achieved by minimizing the quadratic error

$$f_1(\vec{I}_k(\theta_e), \theta_e) = (T_e^{ref} - T_e(\vec{I}_k(\theta_e), \theta_e))^2. \tag{6}$$

Secondly, an additional goal $f_2(\vec{I}_k(\theta_e), \theta_e) \in \mathbb{R}_+$ is selected such that a minimum current magnitude is used to meet the minimum of $f_1(\vec{I}_k(\theta_e), \theta_e)$, so the minimum stator copper loss is produced along with torque ripple mitigation, aiming MTPA operation. This goal is sought by minimizing the current magnitude at each rotor position

$$f_2(\vec{I}_k(\theta_e), \theta_e) = \sum_{p=a,b,c} i_{p,k}^2(\theta_e). \tag{7}$$

Based on (6) and (7) the fitness function $J_1(\vec{I}_k(\theta_e), \theta_e) \in \mathbb{R}_+$ to evaluate each solution candidate can be written as

$$J_1(\vec{I}_k(\theta_e), \theta_e) = \lambda_1 f_1(\vec{I}_k(\theta_e), \theta_e) + f_2(\vec{I}_k(\theta_e), \theta_e) \tag{8}$$

where $\lambda_1 \in \mathbb{R}_+$ is a weight factor controlling the importance of objective $f_1(\vec{I}_k(\theta_e), \theta_e)$ over $f_2(\vec{I}_k(\theta_e), \theta_e)$. The optimized current waveform is obtained when $J_1(\vec{I}_k(\theta_e), \theta_e)$ is minimized by GA over the entire electric cycle. It should be noted that the optimum current waveform depends on load condition, thus, the process needs to be executed to different loading conditions. The Algorithm 1 synthesize the proposed search method for the optimized stator current.

It must be emphasized that the Algorithm 1 performs a free search of a, b and c values of solution candidates with the format of (3)-(5), not imposing constrains other than search space boundaries. The optimized current in this case is denoted by Optimized Current 1 (OC1). On the other hand, considering the imposition of $i_c = -i_a - i_b$, the modified Algorithm 1 will produce an optimized current denoted by Optimized Current 2 (OC2).

A. Numerical Investigations

The nonsinusoidal PMSM considered in this investigation is detailed in the Appendix, whose parameters were obtained by FEA. The parameters of the GA algorithm are shown in Table I. For the optimization process, the electric cycle is divided considering a discretization of 2 electrical and half cycle symmetry. Further, 8 reference torque T_e^{ref} condition were selected to the analysis of each current waveform. Therefore, a total of 720 GA optimizations were performed for each proposed current waveform OC1 and OC2. The resulting OC1 and OC2 current waveforms in an electric cycle for a 6 Nm load condition are shown in Fig. 1 with their respective harmonic distribution, whose magnitudes were normalized with respect to the fundamental component. Different from OC1, the OC2 do not have harmonic components of 3rd and 9th order since the imposition of $i_c = -i_a - i_b$ in the balanced three-phase system.

For the comparison purpose, it is also considered the conventional sinusoidal current aligned to the nonsinusoidal back-EMF, which not benefits the drive with reluctance torque, denoted as zero d-axis current (ZDAC) and conventional MTPA based on sinusoidal stator current [10].

The test PMSM has the 6th torque harmonic as the dominant one under sinusoidal current feeding strategies. Thus, the torque ripple comparison is performed considering only the

Algorithm 1: Pseudo Code for proposed GA approach

```
for Each selected T_e^ref do
    for Each θ_e do
        Initialize random population of P individuals
          I_k(θ_e), with k ∈ 1..P, in the search space M;
        while Termination condition not reached do
            for Each individual I_k(θ_e) do
                Calculate T_e(I_k(θ_e), θ_e) from FEA;
                Evaluate fitness function J_1(I_k(θ_e), θ_e);
            end
            Rank best individuals;
            Select individuals;
            Perform genetic operations on population
              (crossover, mutations & migration) and
              replace the current population with the
              new individuals [17];
        end
        Store the best individual for θ_e, which produces
          min{J_1, k = 1..N} in the last population;
    end
end
```

Table I: **GA parameters**

Description	Type	Value
Selection method	Stochastic Uniform	—
Number of subpopulations	—	2
Subpopulation Size	—	50
Mutation	Gaussian	—
Crossover	Intermediate	0.8
Migration	Unidirectional	20%
Generations between migrations	—	15
Stopping criteria	- Number of generations - Variation of best Fitness value between generations	50 $\leq 10^{-3}$

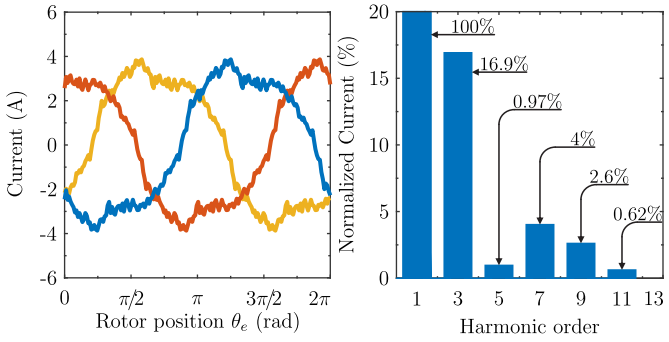

(a) OC1 phase current waveforms.

(b) OC1 harmonic components magnitude.

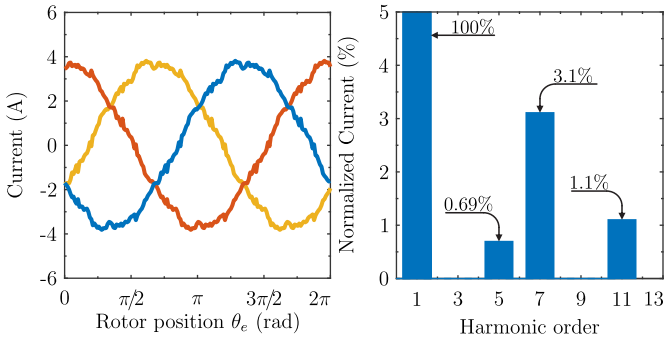

(c) OC2 phase current waveforms.

(d) OC2 harmonic components magnitude.

Figure 1: Optimized current waveforms for torque ripple mitigation at 6 Nm load condition.

amplitude of torque undulation, given by $RT \in \mathbb{R}_+$ defined as

$$RT = \left(\max\{T_e\} - \min\{T_e\}\right) / |T_{avg}| \tag{9}$$

where T_e and $T_{avg} \in \mathbb{R}$ are the electromagnetic torque and its average value in an electric cycle calculated from (1). Fig. 2a compares the torque ripple for the different current strategies considered. As noticed, optimized currents produce null estimated torque ripple while the sinusoidal ZDAC and conventional MTPA achieve 10 to 17%.

From T_{avg} in each strategy, the following torque per Ampère index $\tau \in \mathbb{R}$ is defined

$$\tau = |T_{avg}| / i_{RMS} \tag{10}$$

where $i_{RMS} \in \mathbb{R}_+$ is the RMS value of phase current. Fig. 2b shows a comparison of τ for each strategy in different load conditions, normalized with respect to those developed by ZDAC. As can be noticed, further than benefit the drive with mitigated torque ripple, OC1 provides higher τ than the other current strategies, requiring lower RMS stator currents to develop same average torque. In 3Nm load torque OC1 provides around 2% more τ than the other strategies while in 24Nm it provides 13% more τ than ZDAC, 1% more than OC2 and 0.5% more than sinusoidal MTPA. The overall superior performance of OC1 is due to the significant magnitude of odd multiple of 3rd harmonics in PM flux linkage, whose can contribute in torque production when interacting with the

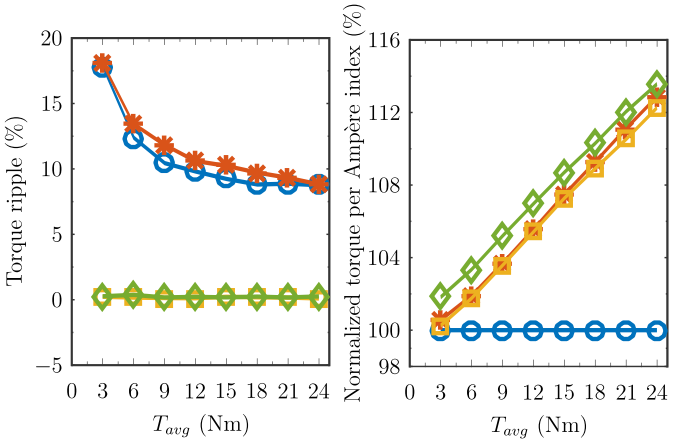

(a) (b)

Figure 2: Torque ripple (a) and τ comparison (b): ZDAC (blue '○' marker); sinusoidal MTPA (orange '*' marker); OC1 (green '◊' marker); OC2 (yellow '□' marker).

respective current harmonics in OC1 [10]. The close τ performance of OC2 and sinusoidal MTPA can be associated to the fact that OC2 requires low magnitude of current harmonics not significantly impacting the current RMS value.

IV. INDUCTANCE VARIATION ANALYSIS

The self and mutual inductances and their derivatives for the different current strategies and load conditions are calculated by means of (2) and the comparison of magnitude variation on the harmonic components N is shown in Fig.3-6. The harmonic magnitudes were normalized with respect to those of no-load condition.

In general, the inductance harmonic magnitudes are modified differently considering the effect of load or the different current strategies. In fact, the load effect can induce the appearance of inductance components with different magnitudes depending on current strategy, as can be seen in Fig. 4a. In most cases, the inductance modification induced by ZDAC is more pronounced than the other strategies. Additionally, similar inductance modification is observed with OC2 and sinusoidal MTPA. This close behavior can be associated to the low harmonic magnitudes required by OC2 to mitigate the torque ripple. On the other hand, OC1 current has higher harmonic magnitudes than OC2 and has induced different inductances modification than OC2 and sinusoidal MTPA in some cases, e.g. 13% decrease in harmonic $N = 4$ of self inductance compared to OC2 and sinusoidal MTPA and 20% compared to ZDAC in 24Nm Fig. 3c.

V. CONCLUSION

Usual proposals in the literature for the design of optimum stator current magnitude/spectrum for torque ripple mitigation are dependent on precise machine electrical parameters. However, these parameters also depend on the stator current, and this mutual dependency imposes a challenge to the problem of torque ripple mitigation. In this paper, we have firstly

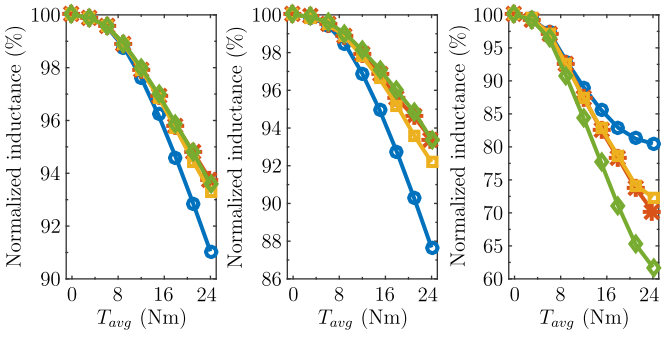

(a) N=0 (b) N=2 (c) N=4

Figure 3: Self inductance variation: ZDAC (blue '○' marker); sinusoidal MTPA (orange '*' marker); OC1 (green '◇' marker); OC2 (yellow '□' marker).

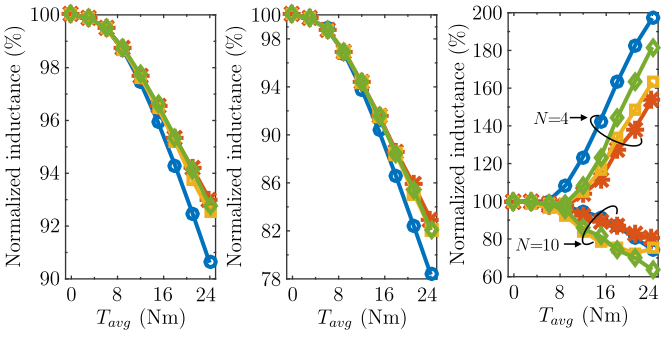

(a) N=0 (b) N=2 (c) N=4 and N=10

Figure 5: Mutual inductance variation: ZDAC (blue '○' marker); sinusoidal MTPA (orange '*' marker); OC1 (green '◇' marker); OC2 (yellow '□' marker).

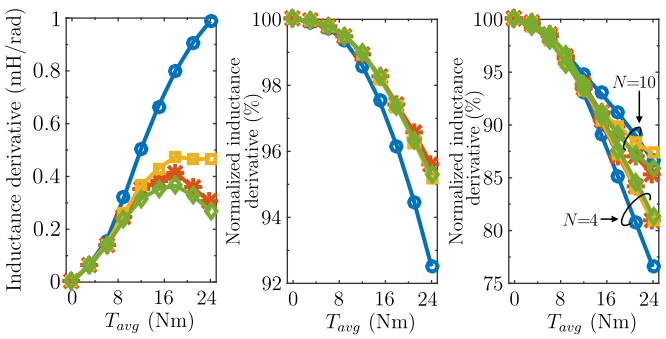

(a) N=0 (b) N=2 (c) N=4 and N=10

Figure 4: Self inductance derivative variation: ZDAC (blue '○' marker); sinusoidal MTPA (orange '*' marker); OC1 (green '◇' marker); OC2 (yellow '□' marker).

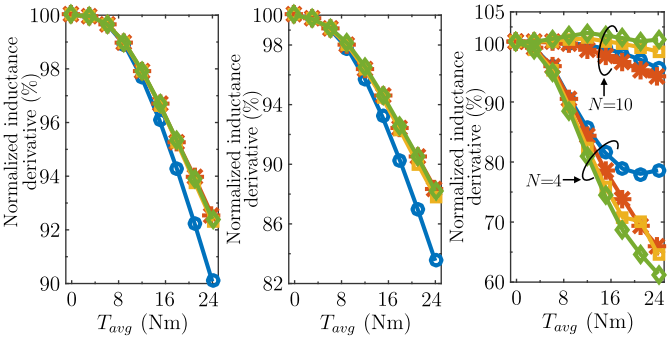

(a) N=0 (b) N=2 (c) N=4 and N=10

Figure 6: Mutual inductance derivative variation: ZDAC (blue '○' marker); sinusoidal MTPA (orange '*' marker); OC1 (green '◇' marker); OC2 (yellow '□' marker).

presented a GA based search method assisted by FEA for design and mapping of optimized stator currents to mitigate torque ripple with minimum current magnitude on a PMSM with spatial harmonics in inductances, PM flux and cogging torque. The method was employed to provide optimized currents with and without zero sequence components utilization since it presents important zero sequence harmonic magnitude on PM flux. An advantage of proposed method compared to earlier works is that it does not depend on machine electrical parameters and inherently accounts for the machine saturation because it is based on the machine design and MST/FPM analysis.

Once the optimized currents are obtained, this paper presents a FEA based investigation of the on-load machine inductance parameters variation considering conventional sinusoidal and the optimized nonsinusoidal stator currents. The results have emphasized that the current waveform differently modifies the parameters under saturation, demonstrating the difficulty of optimum current design from parametric model.

The optimum current search method combined to the parameters calculation presented in this paper are based on the FEA of the machine design. Therefore, it can be performed on the early stages of a drive conceiving and can be extended to other machine topologies, serving as a prior stage to the implementation of analytical model based torque ripple mitigation control strategies. Future research efforts will investigate the current design for torque ripple mitigation in open phase fault operation condition and extend the investigation of parameter variation considering PM flux linkage and cogging torque under different current strategies.

APPENDIX

The PMSM cross section model is exhibited in Fig. 7. From the FEA simulation and the improved methods in [12], [13], [16], the no-load machine parameters are shown in Fig. 8 together with their harmonic spectrum, in which the harmonic components are normalized with respect to the lowest order harmonic magnitude.

ACKNOWLEDGMENT

The authors would like to thank the financial support granted by National Council of Research and Development (CNPq), Coordenação de Aperfeiçoamento de Pessoal de Nível Superior - Brasil (CAPES) - Finance Code 001, Goiás

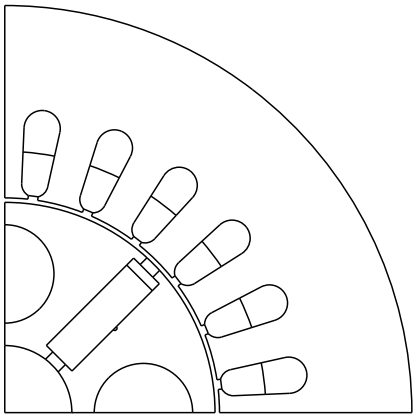

Figure 7: PMSM cross section model view.

Table II: **Parameters of the PMSM**

Parameter	Value		Parameter	Value	
Stator Outer Diameter	182	mm	Tooth Width	8.16	mm
Stator Inner Diameter	96	mm	Slot Opening	2.2	mm
Stator Yoke	22.9	mm	Shaft Diameter	30	mm
Airgap	1	mm	Tooth Shoes	1	mm
Rotor Outer Diameter	47	mm	PM Type	NdFeB	
Slots	24		PM Thickness	8.3	mm
Poles	4		Coil Turns	38	
Stack Length	102	mm	Skew angle	24°	

Research Foundation (FAPEG), and São Paulo Research Foundation (FAPESP), grant #2006/04226-0.

REFERENCES

[1] D.-K. Kim, K.-W. Lee, and B.-I. Kwon, "Commutation Torque Ripple Reduction in a Position Sensorless Brushless DC Motor Drive," *IEEE Trans. Power Electron.*, vol. 21, no. 6, pp. 1762–1768, nov 2006.

[2] M. Melfi, S. Evon, and R. McElveen, "Induction versus permanent magnet motors," *IEEE Ind. Appl. Mag.*, vol. 15, no. 6, pp. 28–35, nov 2009.

[3] Z. Q. Zhu and D. Howe, "Electrical Machines and Drives for Electric, Hybrid, and Fuel Cell Vehicles," *Proc. IEEE*, vol. 95, no. 4, pp. 746–765, 2007.

[4] Z. Q. Zhu and J. H. Leong, "Analysis and mitigation of torsional vibration of PM brushless AC/DC drives with direct torque controller," *IEEE Trans. Ind. Appl.*, vol. 48, no. 4, pp. 1296–1306, 2012.

[5] P. Beccue, J. Neely, S. Pekarek, and D. Stutts, "Measurement and Control of Torque Ripple-Induced Frame Torsional Vibration in a Surface Mount Permanent Magnet Machine," *IEEE Trans. Power Electron.*, vol. 20, no. 1, pp. 182–191, jan 2005.

[6] T. Jahns and W. Soong, "Pulsating torque minimization techniques for permanent magnet AC motor drives-a review," *IEEE Trans. Ind. Electron.*, vol. 43, no. 2, pp. 321–330, apr 1996.

[7] N. Bianchi, M. Degano, and E. Fornasiero, "Sensitivity analysis of torque ripple reduction of synchronous reluctance and interior PM motors," *IEEE Trans. Ind. Appl.*, vol. 51, no. 1, pp. 187–195, 2015.

[8] A. J. Ortega and L. Xu, "Analytical prediction of torque ripple in surface-mounted permanent magnet motors due to manufacturing variations," *IEEE Trans. Energy Convers.*, vol. 31, no. 4, pp. 1634–1644, 2016.

[9] C. Lai, G. Feng, K. Lakshmi Varaha Iyer, K. Mukherjee, and N. C. Kar, "Genetic Algorithm-Based Current Optimization for Torque Ripple Reduction of Interior PMSMs," *IEEE Trans. Ind. Appl.*, vol. 53, no. 5, pp. 4493–4503, 2017.

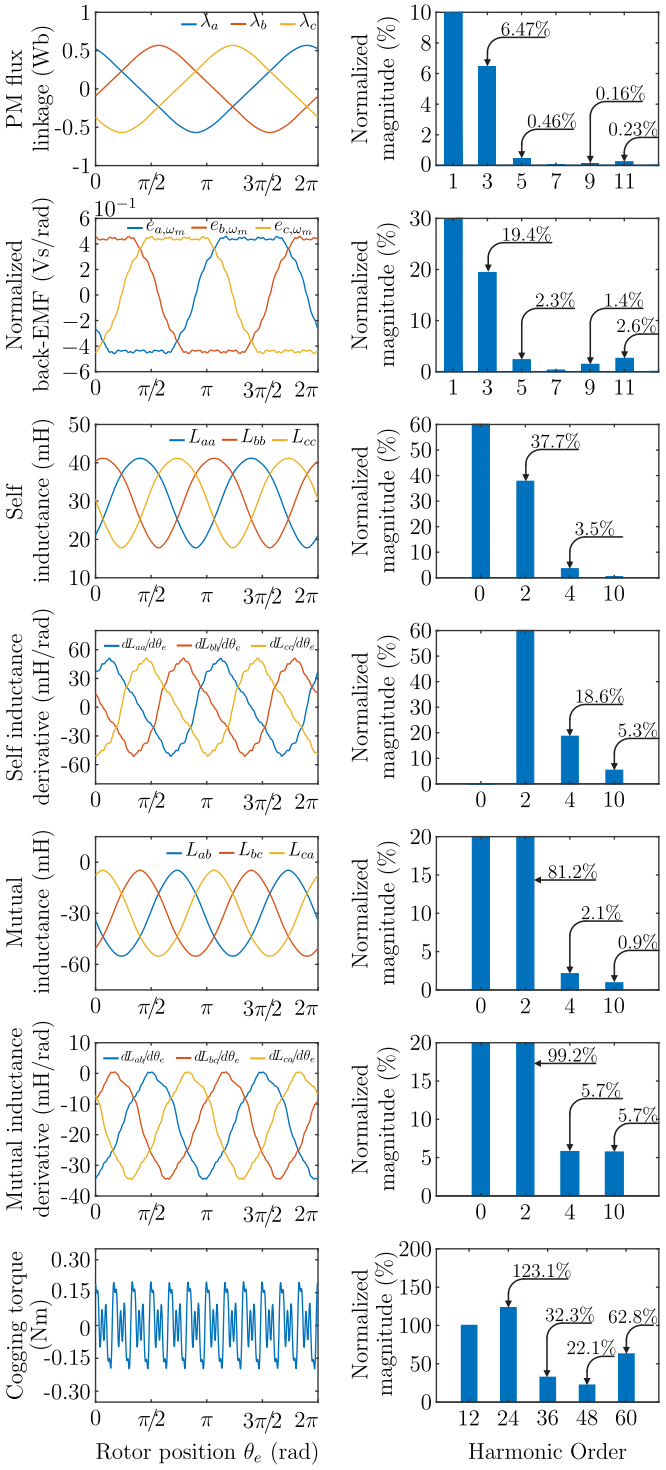

Figure 8: No-load machine electrical parameters.

[10] A. G. D. Castro, P. R. U. Guazzelli, C. M. R. D. Oliveira, W. C. A. Pereira, G. D. Paula, and J. R. B. A. Monteiro, "Optimized Current Waveform for Torque Ripple Mitigation and MTPA Operation of PMSM with Back-EMF Harmonics based on Genetic Algorithm and Artificial Neural Network," *IEEE Lat. Am. Trans.*, 2020.

[11] G. Feng, C. Lai, and N. C. Kar, "An Analytical Solution to Optimal Stator Current Design for PMSM Torque Ripple Minimization With Minimal Machine Losses," *IEEE Trans. Ind. Electron.*, vol. 64, no. 10,

pp. 7655–7665, oct 2017.
[12] G. T. De Paula, J. R. B. De Monteiro, B. P. De Alvarenga, T. E. De Almeida, W. C. Pereira, and M. P. De Santana, "On-Load Back EMF of PMSM Using Maxwell Stress Tensor," *IEEE Trans. Magn.*, vol. 54, no. 7, 2018.
[13] C. Filho, B. P. De Alvarenga, and G. T. De Paula, "On-Load Apparent Inductance Derivative of IPMSM: Assessment Method and Torque Estimation," *IEEE Trans. Magn.*, vol. 56, no. 4, 2020.
[14] C. Filho, L. Assis, B. Alvarenga, and G. T. de Paula, "Influence of Vector Control Strategies on Magnetic Saturation and its Effects on Torque Ripple of a PMSM," in *2018 13th IEEE Int. Conf. Ind. Appl.* IEEE, nov 2018, pp. 1051–1058.
[15] N. Sadowski, Y. Lefevre, M. Lajoie-Mazenc, and J. Cros, "Finite element torque calculation in electrical machines while considering the movement," *IEEE Trans. Magn.*, vol. 28, no. 2, pp. 1410–1413, mar 1992.
[16] L. F. D. Assis, C. C. L. Filho, G. T. D. Paula, and B. P. D. Alvarenga, "Comparative Analysis of Different Methods Associated to the Frozen Permeability Method for On-Load Cogging Torque Evaluation in Permanent Magnet Synchronous Machines," *IEEE Lat. Am. Trans.*, 2020.
[17] M. Mitchell, *An introduction to genetic algorithms*. MIT Press, 1996.
[18] S. Sheng and Z. Dechen, "Genetic algorithm for the transportation problem with discontinuous piecewise linear cost function," *Int. J. Comput.*, vol. 6, no. 7A, pp. 182–190, 2006.